CAPACITY AND POSITIONING IN DENSE SCATTERING ENVIRONMENTS

Nadia Fawaz, David Gesbert

Mobile Communications Department, Eurecom Institute
Sophia-Antipolis, France
{fawaz, gesbert}@eurecom.fr

Merouane Debbah

Supélec
Gif-sur-Yvette, France
merouane.debbah@supelec.fr

ABSTRACT

We study the capacity scaling of a system where a source communicates to a destination with the help of several scatterers. Capacity expressions accounting for physical characteristics of the environment (topology, frequency band...) are provided and an asymptotic analysis is performed for an increasing size of the dense scattering environment. The capacity is shown to reach a saturation level in the asymptotic regime, suggesting a capacity-delay trade-off. Moreover the saturation point depends on the positioning of scatterers, in particular in wide band systems where topology impacts capacity in terms of both pathloss and delays. Waiting very long for retransmissions from an infinite number of scatterers is not worth and a few well located scatterers around source and destination lead to better performances than more scatterers uniformly distributed on a square area between source and destination.

1. INTRODUCTION

The issue of how the performance of virtual MIMO systems scale with the number of nodes or size of a network is a crucial issue. It may turn out that virtual MIMO is only adapted for short range communications and therefore that some kind of hybrid virtual MIMO scheme with base stations and ad-hoc networks will arise as the most convenient scheme. Since the pioneering work by Gupta and Kumar [1] providing the capacity of a large ad hoc network with several Source-Destination pairs, several recent works [2], [3] studied capacity scaling laws in large narrow-band networks: [2] proposed a hierarchical cooperation protocol to achieve linear scaling of capacity in the number of single-antenna nodes randomly distributed in an area, whereas the protocol in [3], for cooperation between M-antenna source, destination and K relays inbetween, leads to a capacity scaling as $C = (M/2)\log K + O(1)$. Nevertheless to the best of our knowledge, no previous work focused on the scaling of capacity in dense wideband – thus with high resolution in time and space – networks of dumb scatterers taking into account topology not only in terms of pathloss but also of multi-path. Moreover the environment impact on the scaling laws, through reflections, diffraction effects... has never been studied in details, although this aspect is used for example in MIMO communications to create different spatial multiplexing streams. We would like here to go deeper in the analysis.

In this paper we analyze a system where a dense topology of scatterers helps a source to communicate with a destination and we look at the network from a physical propagation point of view : relays are modeled as dumb omnidirectional scatterers, i.e. passive nodes without engineering capabilities that simply scatter the incident electromagnetic wave coming from source antenna. Capacity expressions are given as a function of the physical characteristics of the network, including topology and signal band. We study how capacity scales when the size the network increases, as well as the point at which asymptotic regime is reached depending on the nodes positioning. Interestingly the asymptotic analysis, and simulations in wideband systems, show that after a certain point, capacity saturation occurs. This is due to the fact that signal contributions coming from peripheral nodes very far from source and destination do not lead to much increased performance, suggesting a capacity/delay trade-off, which may not be the case when adding MIMO capability.

The rest of the paper is organized as follows. In section 2, the network model is described before deriving the network capacity in section 3. Numerical results are provided in section 4 and lead to the concluding section 5.

2. SYSTEM MODEL

We focus on a geometrical network model by considering a finite square grid of scatterers, spaced by $\lambda_s/2 = c/(2W)$ vertically and horizontally, where W is the sampling rate. Source S and Destination D are located on vertices of the grid separated by a distance $d_0 = m\lambda_s/2$. The carrier wavelength will be denoted $\lambda_c = c/f_c$.

2.1. Scatterers Clustering

In a wide band system, resolution in time and space are high and propagation delays cannot be neglected as in narrow band

The work of Nadia Fawaz is supported by a grant from the French Defense Body, DGA and by BIONETS projects (FP6-027748, www.bionets.eu).

systems. Indeed λ_s may be small compared to the distance between communicating terminals, therefore a signal transmitted during a given time-slot will not be received in the same time-slot but later. To take into account propagation delays, scatterers are grouped in N_{clus} clusters, depending on the time-slot of reception of the scattered wave.

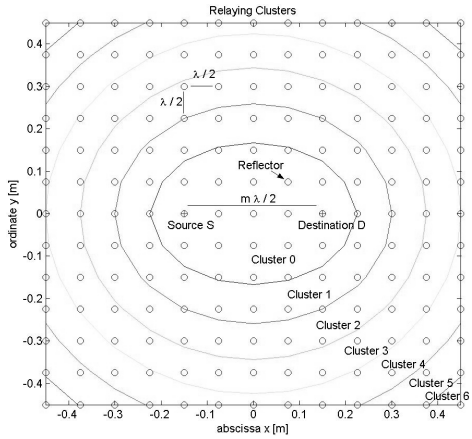

Fig. 1. Relaying Clusters

If we sample at $W = c/\lambda_s$, we can discriminate durations greater than the time $T = \lambda_s/c$ needed by the wave to propagate along λ_s meters. Thus a cluster gathers scatterers whose scattered waves are received by D during the same interval T.

The shortest distance to go from source to destination is the straight path without reflection of length d_0 and propagation duration $\tau_0 = d_0/c = (m/2)T$. Cluster Δ_0 contains the straight path from source to destination, as well as the reflected paths received during the first time-slot $TS_0 = [\tau_0, \tau_0 + T[$. Those paths correspond to waves propagating on a total distance, sum of the distances from S to the scatterer and from the scatterer to D, $d_r^{(s)} + d_r^{(d)} \in [d_0, d_0 + \lambda_s[$. For $i \geq 1$, Cluster Δ_i contains only scattered waves, such that $(d_r^{(s)} + d_r^{(d)}) \in [d_0 + i\lambda_s, d_0 + (i+1)\lambda_s[$. Those waves are received during the i^{th} time-slot defined by $TS_i = [\tau_0 + iT, \tau_0 + (i+1)T[$. For a scatterer k in cluster i, the propagation delay of the scattered wave from S to D via this scatterer $R_{k,i}$ will be denoted $\tau_{k,i} \in TS_i$. This duration consists of three parts: $\tau_{k,i} = \tau_0 + iT + \tau'_{k,i}$ with $\tau'_{k,i} \in [0, T[$.

Fig. (1) illustrates the clusters in the case of a 13×13 grid and a source-destination distance $d_0 = 4\ \lambda_s/2$. A cluster is geometrically represented by a surface bounded by two ellipses whose focus are S and D, and whose equations are given by $d_r^{(s)} + d_r^{(d)} = d_0 + i\lambda_s$ and $d_r^{(s)} + d_r^{(d)} = d_0 + (i+1)\lambda_s$.

2.2. Power Attenuation

To model the attenuation of propagating waves, the far field propagation model holding for distances $d \gg \frac{\lambda_c}{2\,\pi}$ will be considered. Since $f_c \geq W/2 \Leftrightarrow \lambda_s \geq \lambda_c/2$, the far field condition is fulfilled for distances $d \geq \lambda_s/2$. The power received by D depends on the path taken by the signal to reach D: one-hop direct path from S to D without reflection or two-hop-path from S to D via one scatterer. Multiple reflections before reaching D are not taken into account.

If no reflection occurs, the direct received power [4, 5] is :

$$P_d = \frac{\lambda_c^2}{(4\pi)^2\ d_0^2}\ P_{rad} = K_1^2 \frac{\lambda_c^2}{d_0^2}\ P_{rad} \qquad (1)$$

with P_{rad} the power transmitted by the source antenna and the constant $K_1 = 1/(4\pi)$. If one reflection occurs before reaching D, according to the radar equation [4, 5] with omni-directional antennas, the reflected power received by D is:

$$P_r = \frac{\lambda_c^2\ s}{(4\pi)^3\ (d_r^{(s)}\ d_r^{(d)})^2}\ P_{rad} = K_2^2\ \frac{\lambda_c^2}{(d_r^{(s)}\ d_r^{(d)})^2}\ P_{rad} \quad (2)$$

with s the radar cross section and $K_2 = \sqrt{s/4\pi} K_1 = \sqrt{s/(4\pi)^3}$.

3. ANALYSIS

Matrices and vectors are represented by boldface uppercase. $\mathbf{A}^T, \mathbf{A}^*, \mathbf{A}^H$ denote the transpose, the conjugate and the transpose conjugate of matrix $\mathbf{A}$ whereas operator $*$ stands for convolution. $\det(\mathbf{A})$ stands for determinant of $\mathbf{A}$, $\mathbb{E}$ is statistical expectation and finally $\mathbf{I}_N$ is the identity matrix of size N.

3.1. Signals Expressions in Time Domain

Source S produces a sequence $s(t) = \sum_{n=0}^{N-1} s_n\ \delta(t - nT)$ of N complex symbols with unit energy $\varepsilon = E[|s_n^2|] = P_{rad}$ at rate $W = 1/T$ and transmits a linearly modulated signal with complex envelope $x(t) = s(t) * g(t) = \sum_{n=0}^{N-1} s_n\ g(t - nT)$, where $g(t)$ is the pulse shaping filter, satisfying the Nyquist criterion $\int g(t)g^*(t - kT)dt = \delta_{0,k}$. We assume hereafter that $g(t)$ is the rectangle function of amplitude $1/\sqrt{T}$ over $[0, T[$. The received signal at D is the superposition of the signal coming directly from S and the signals scattered once:

$$y(t) \quad = \quad \sum_{i=0}^{N_{clus}-1} \sum_{k \in \Delta_i} a_{k,i}\ x(t - \tau_{k,i}) \ +\ n'(t) \qquad (3)$$

where n'(t) is AGWN and coefficients $a_{k,i}$ are given by (1) and (2):

$$a_{k,i} = \begin{cases} K_1 \frac{\lambda_c}{d_0} e^{j\varphi_{0,0}} & \text{for } (k,i) = (0,0) \quad \text{direct path} \\ K_2 \frac{\lambda_c}{d_{k,i}^{(s)}\ d_{k,i}^{(d)}} e^{j\varphi_{k,i}} & \text{for } (k,i) \neq (0,0) \quad \text{reflected path} \end{cases}$$

$\varphi_{k,i} \in [0, 2\pi[$ are phase shifts due to propagation and reflections. Phases can be modeled as independent random variables provided nodes are sufficiently spaced. If the network becomes denser and denser, phases may not be independent

anymore but correlated and should be expressed in function of optical path differences, which is out of the scope of this paper. After matched-filtering, the received signal becomes:

$$\begin{aligned} r(t) &= y(t) * g^*(-t) \; + \; n(t) \\ &= s(t) * \underbrace{g(t) * g^*(-t) * \sum_{i=0}^{N_{clus}-1} \sum_{k \in \Delta_i} a_{k,i} \, \delta(t - \tau_{k,i})}_{h(t-\tau_0)} \; + n(t) \\ r(t) &= h(t) * s(t - \tau_0) \; + \; n(t) \end{aligned} \quad (4)$$

where we define the scatterers network equivalent channel by:

$$h(t) = \sum_{i=0}^{N_{clus}-1} \sum_{k \in \Delta_i} a_{k,i} \, g(t - \tau_{k,i} + \tau_0) * g^*(-t) \quad (5)$$

Time shift τ_0 in equation (4) illustrates the minimum propagation delay corresponding to direct path. D starts receiving signals only τ_0 seconds after S started emitting. The introduction of τ_0 in the definition of h simplifies notations since all the delays $\tau_{k,i} = \tau_0 + iT + \tau'_{k,i}$ contain τ_0.

By sampling at rate $W = 1/T$, the received sequence is the convolution between the symbol sequence and the channel impulse response (CIR):

$$\begin{aligned} r_l &= r(lT) = \sum_{n=0}^{N-1} s_n h(lT - nT - \tau_0) + n(lT) \quad (6) \\ &= \sum_{n=0}^{N-1} s_n h_{l-n-m/2} + n_l = \sum_{n=0}^{N_{clus}} h_n \, s_{l-n-m/2} + n_l \end{aligned}$$

The sum in (6) is finite and contains only $N_{clus} + 1$ non null terms, since the CIR has finite length $N_{clus} + 1$ (proof and coefficient h_l expression in appendix A). Because of the minimum propagation delay $\tau_0 = mT/2$, the $m/2$ first samples $r_0 = ...r_{m/2-1} = 0$ are null.

Under matrix notation, the system can be reduced to the equation $\mathbf{R}_N = \mathbf{H}_N \mathbf{S}_N + \mathbf{N}_N$, where $\mathbf{S}_N = [s_0, ..., s_{N-1}]^T$, $\mathbf{N}_N = [n_0, ..., n_{N-1}]^T$, $\mathbf{R}_N = [r_{m/2}, ..., r_{N+m/2-1}]^T$ are columns of size N and the channel is represented by $N \times N$ lower triangular banded Toeplitz matrix :

$$\mathbf{H}_N = \begin{bmatrix} h_0 & 0 & \dots & \dots & \dots & 0 \\ \vdots & \ddots & \ddots & & & \vdots \\ h_{N_{clus}} & & \ddots & \ddots & & \vdots \\ 0 & \ddots & & \ddots & \ddots & \vdots \\ \vdots & \ddots & \ddots & & \ddots & 0 \\ 0 & \dots & 0 & h_{N_{clus}} & \dots & h_0 \end{bmatrix}_{N \times N} \quad (7)$$

3.2. Asymptotic analysis for Capacity expression

The capacity of the grid of scatterers is defined [6] as:

$$C = \lim_{N \to +\infty} \frac{W}{N} \log_2 \det \left(\mathbf{I}_N + \frac{\varepsilon}{W\sigma^2} \mathbf{H}_N \mathbf{H}_N^H \right) \quad (8)$$

Using Toeplitz and circulant matrices properties, we show in appendix B that:

$$C = \lim_{N \to +\infty} \frac{W}{N} \sum_{k=0}^{N-1} \log_2 (1 + \frac{\varepsilon}{W\sigma^2} |\lambda_{k,N}|^2) \quad (9)$$

where $\{\lambda_{k,N}\}_{k \in [0,N-1]}$ are given by the N-point DFT of the first column of $\mathbf{H}_N$.

Expressing the average capacity in terms of the network physical characteristics is intricate. Nevertheless Jensen's inequality allows to give an upperbound (10) to the average capacity $\bar{C} = \mathbb{E}_h[C]$ in function of physical characteristics of the network. Besides at low SNR $\rho = \frac{\varepsilon}{\sigma^2}$, using Taylor expansion of the log around zero at order 1 and performing some tedious manipulations of (8), that we skip for sake of conciseness and readability, $\bar{C}$ can be written as in (11). They illustrate the SNR gain due to scatterers in function of the topology and the system band . We would like to point out that those formulas are valid for any topology and are not specific to the grid model, nor to the $\lambda_s/2$-node spacing.

4. SIMULATIONS AND RESULTS

In this section, numerical results illustrate the growth of average capacity when the number of scatterers increases. We consider a wide band system with $W = 2GHz$ and a carrier $f_c = 2GHz$, at SNR $\rho = 10dB$, for different values of distance d_0. Scatterers are located on the vertices of a square grid covering an area of $21\lambda_s/2 \times 21\lambda_s/2$. Nevertheless we consider that the line (SD) does not contain any scatterer, since when three nodes are aligned, one link among the links S-R, S-D, R-D is blocked.

The number of scatterers is increased in two different ways:

- **Centered-Grid Positioning** : N_r scatterers are uniformly distributed on the vertices of a grid of size $\sqrt{N_r} \times \sqrt{N_r}$, centered on the midpoint I between S and D. Increasing N_r corresponds to increasing the edge of the square grid. The average capacity (9) obtained by Monte-Carlo simulations over many independent channel realizations as well as Jensen's upperbound (10) are plotted in fig. (2) for the centered grid positioning.

- **Optimal Positioning** : Considering a grid 21×21, we select the N_r optimal vertices , i.e. the positions that give the highest capacity for a given number N_r of scatterers. Increasing N_r corresponds to adding a scatterer at the available vertex which gives the next highest increase of capacity. Jensen's upperbound (10) only is plotted in this case in fig. (2).

As the number of scatterers increases, capacity saturation occurs, since signals coming from peripheral nodes very far from source and destination lead to small contributions, suggesting a capacity/delay trade-off: after a certain point, the

$$\bar{C} \leq W \log\left(1 + \frac{\rho}{W}\left(K_1^2\frac{\lambda_c^2}{d_0^2} + K_2^2\frac{\lambda_c^2}{\lambda_s^2}\sum_{i=0}^{N_{clus}-1}\sum_{k\in\Delta_i}\frac{((i+1)\lambda_s + d_0 - d_{k,i}^{(s)} - d_{k,i}^{(d)})^2 + (i\lambda_s + d_0 - d_{k,i}^{(s)} - d_{k,i}^{(d)})^2}{(d_{k,i}^{(s)} d_{k,i}^{(d)})^2}\right)\right) \quad (10)$$

$$\text{At low SNR: } \bar{C} \approx \frac{\rho}{\ln 2}\left(K_1^2\frac{\lambda_c^2}{d_0^2} + K_2^2\frac{\lambda_c^2}{\lambda_s^2}\sum_{i=0}^{N_{clus}-1}\sum_{k\in\Delta_i}\frac{((i+1)\lambda_s + d_0 - d_{k,i}^{(s)} - d_{k,i}^{(d)})^2 + (i\lambda_s + d_0 - d_{k,i}^{(s)} - d_{k,i}^{(d)})^2}{(d_{k,i}^{(s)} d_{k,i}^{(d)})^2}\right) \quad (11)$$

increase in capacity resulting from retransmissions from far nodes is not worth the time wasted waiting for those retransmissions. With respect to the case without scatterers, the level of saturation corresponds to a 30% increase in capacity at $d_0 = 3\lambda_s$ and 40% at $d_0 = 5\lambda_s$.

Fig. 3 shows how the contribution to SNR of each scatterer depends on its position. Scatterers positions affect the capacity not only in terms of path loss but also of delay, leading to a notable difference between performances in the centered-grid case and the optimal positioning case. A few scatterers well located, close to source or destination according to fig. (3), lead to better performances than a great number of scatterers uniformly distributed between source and destination.

5. CONCLUSION

In this contribution, the scaling behavior of capacity in a dense scattering network is analyzed from a physical point of view, taking into account characteristics such as topology and transmission band. Asymptotic analysis shows that capacity saturates when the size of the network increases and that topology affects the saturation point, in particular in wide band systems where the impact of topology on capacity is not only a matter of pathloss but also of delays that cannot be neglected. Capacity saturation suggests a capacity/delay trade-off : it is not worth waiting for infinite retransmissions and a few well located scatterers around source and destination lead to better performances than more scatterers uniformly distributed on a square area centered between source and destination.

A. PROOF OF FINITE LENGTH OF CIR

The channel impulse response is defined by the coefficients:

$$h_l = h(lT) = \sum_{i=0}^{N_{clus}-1}\sum_{k\in\Delta_i} a_{k,i}\int g(\tau - \tau_{k,i} + \tau_0) g^*(\tau - lT)d\tau \quad (12)$$

By definition with a rectangle transmitting filter, the integral in (12) is non null for a finite set of values of l, more precisely $l \in [0, N_{clus}]$, as shown hereunder:

$$\begin{aligned} & \int g(\tau - \tau_{k,i} + \tau_0)\, g^*(\tau - lT)d\tau \\ = \;& \int g(\tau)\, g^*(\tau + \tau'_{k,i} - (l-i)T)d\tau \\ = \;& f_{k,l}^{(1)}\,\delta_{i-l} + f_{k,l-1}^{(2)}\,\delta_{i-l-1} \end{aligned} \quad (13)$$

with $\tau'_{k,i} \in [0, T[$, and $f^{(1)}$ and $f^{(2)}$ are defined by:

$$\text{for} \quad i \in [0, N_{clus}-1] \text{ and } k \in \Delta_i,$$

$$f_{k,i}^{(1)} = \int g(\tau)\, g^*(\tau + \tau'_{k,i})d\tau = 1 - \tau'_{k,i}/T \quad (14)$$

$$f_{k,i}^{(2)} = \int g(\tau)\, g^*(\tau - T + \tau'_{k,i})d\tau = \tau'_{k,i}/T \quad (15)$$

Then combining (12) and (13) leads to the coefficients:

$$\begin{aligned} h_0 &= h_0^{(1)} = \sum_{k\in\Delta_0} a_{k,0}\, f_{k,0}^{(1)} \\ h_l &= h_l^{(1)} + h_{l-1}^{(2)} \quad \text{, for } l \in [1, N_{clus}-1] \\ &= \sum_{k\in\Delta_l} a_{k,l}\, f_{k,l}^{(1)} + \sum_{k\in\Delta_{l-1}} a_{k,l-1}\, f_{k,l-1}^{(2)} \\ h_{N_{clus}} &= h_{N_{clus}-1}^{(2)} = \sum_{k\in\Delta_{N_{clus}-1}} a_{k,N_{clus}-1}\, f_{k,N_{clus}-1}^{(2)} \end{aligned} \quad (16)$$

Indeed, h is the superposition of two FIR $h^{(1)}$ and $h^{(2)}$, of length $N_{clus}-1$, shifted by T with respect to each other. Thus, h is of length N_{clus}.

B. PROOF OF CAPACITY EXPRESSION (9)

$\{\mathbf{H}_N\}_{N\in\mathbb{N}}$ forms a sequence of banded Toeplitz matrices of order $N_{clus}+1$ (non null coefficients). We study their asymptotic behavior, i.e. for $N \gg N_{clus}$. As in [7] we define:

- the circulant matrix $\mathbf{G}_N$ associated to $\mathbf{H}_N$:

$$\mathbf{G}_N = \begin{bmatrix} h_0 & 0 & \dots & 0 & h_{N_{clus}} & \dots & h_1 \\ \vdots & \ddots & \ddots & & \ddots & \ddots & \vdots \\ h_{N_{clus}} & & \ddots & \ddots & & \ddots & h_{N_{clus}} \\ 0 & \ddots & & \ddots & \ddots & & 0 \\ \vdots & \ddots & \ddots & & \ddots & \ddots & \vdots \\ \vdots & & \ddots & \ddots & & \ddots & 0 \\ 0 & \dots & \dots & 0 & h_{N_{clus}} & \dots & h_0 \end{bmatrix}_{N\times N}$$

- the sequence $\{\mathbf{A}_N\}_{N\in\mathbb{N}}$ of hermitian matrices $\mathbf{A}_N = \mathbf{H}_N\mathbf{H}_N^H$ with non negative eigenvalues sets $\{\alpha_{k,N}\}_{k\in[0,N-1]}$
- the sequence $\{\mathbf{B}_N\}_{N\in\mathbb{N}}$ of hermitian matrices $\mathbf{B}_N = \mathbf{G}_N\mathbf{G}_N^H$ with non negative eigenvalues sets $\{\beta_{k,N}\}_{k\in[0,N-1]}$

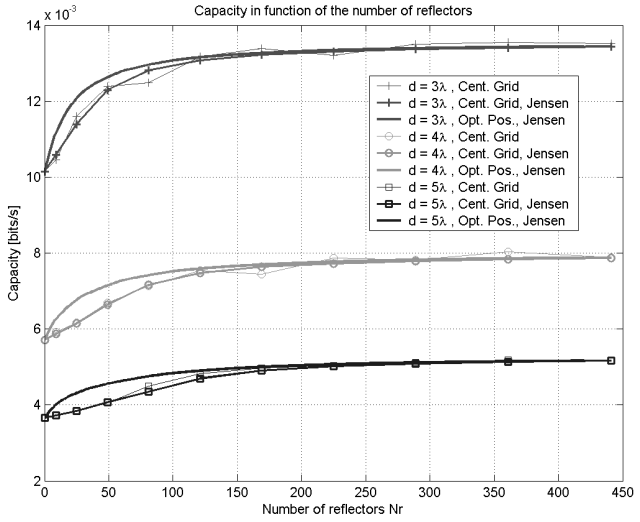

Fig. 2. Capacity in function of the number of scatterers

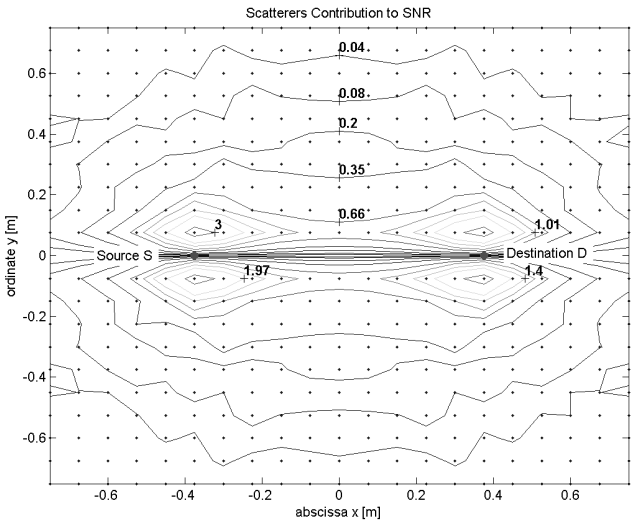

Fig. 3. Contribution to SNR of scatterers vs. their position

According to lemma 4.2 in [7], $\mathbf{H}_N$ and $\mathbf{G}_N$ are asymptotically equivalent, as well as $\mathbf{H}_N^H$ and $\mathbf{G}_N^H$. Thus, by theorem 2.1.(3) in [7], their products are asymptotically equivalent: $\mathbf{A}_N = \mathbf{H}_N\mathbf{H}_N^H \sim \mathbf{G}_N\mathbf{G}_N^H = \mathbf{B}_N$ and by theorem 2.1.(6), there are finite constant m and M such that $m \leq \alpha_{k,N}, \beta_{k,N} \leq M$. In particular $\mathbf{A}_N$ and $\mathbf{B}_N$ are nonnegative definite, so $0 \leq \alpha_{k,N}, \beta_{k,N} \leq M$.

The capacity (8) can be written:

$$C = \lim_{N\to+\infty} \frac{W}{N} \sum_{k=0}^{N-1} \log_2(1 + \frac{\varepsilon}{W\sigma^2}\alpha_{k,N}) \quad (17)$$

From (17) we define the function $F(u) = \log_2(1 + \frac{\varepsilon}{W\sigma^2}u)$, continuous on $]-\frac{W\sigma^2}{\varepsilon}, +\infty[$ and thus on the interval $[0, M]$ bounding the eigenvalues $\alpha_{k,N}$ and $\beta_{k,N}$. $\{\mathbf{A}_N\}_{N\in\mathbb{N}}$ and $\{\mathbf{B}_N\}_{N\in\mathbb{N}}$ being asymptotically equivalent sequences of hermitian matrices, theorem 2.4 of [7] allow to conclude that:

$$\lim_{N\to+\infty} \frac{1}{N} \sum_{k=0}^{N-1} F(\alpha_{k,N}) = \lim_{N\to+\infty} \frac{1}{N} \sum_{k=0}^{N-1} F(\beta_{k,N}) \quad (18)$$

and rewrite the capacity (17):

$$C = \lim_{N\to+\infty} \frac{W}{N} \sum_{k=0}^{N-1} \log_2(1 + \frac{\varepsilon}{W\sigma^2}\beta_{k,N}) \quad (19)$$

Now $\mathbf{G}_N$ is a circulant matrix, thus diagonalizable in the Fourier basis, leading to the diagonal matrix $\mathbf{C}_N = \mathbf{F}_N\mathbf{G}_N\mathbf{F}_N^{-1} = diag(\lambda_{0,N}, \ldots, \lambda_{N-1,N})$ and the eigenvalues $\{\lambda_{k,N}\}_{k\in[0,N-1]}$ given by the DFT of the first column of $\mathbf{G}_N$:

$$[\lambda_{0,N}, ..., \lambda_{N-1,N}]^T = \mathbf{F}_N\,[h_0, ..., h_{N_{clus}-1}, 0, ..., 0]^T_{(N\times 1)}$$

where $\mathbf{F}_N = (e^{-\frac{j2\pi(n-1)(\nu-1)}{N}})_{n,\nu\in\{1...N\}}$ is the N-point DFT matrix. Expressing $\mathbf{B}_N$ in function of $\mathbf{C}_N$ gives

$$\mathbf{B}_N = \mathbf{F}_N^{-1}\mathbf{C}_N\mathbf{C}_N^H\mathbf{F}_N = \mathbf{F}_N^{-1}diag(|\lambda_{0,N}|^2, \ldots, |\lambda_{N-1,N}|^2)\mathbf{F}_N$$

so that $\beta_{k,N} = |\lambda_{N,k}|^2$, which substituted in (19) leads (9).

C. REFERENCES

[1] P. Gupta and P.R. Kumar, "The capacity of wireless networks," *IEEE Trans. Inform. Theory*, vol. 46, no. 2, pp. 388–404, Mar. 2000.

[2] A. Özgür, O. Lévêque, and D. Tse, "How does the information capacity of ad hoc networks scale?," in *Proc. 44th Annual Allerton Conference on Communication, Control, and Computing*, Sept. 2006.

[3] H. Bolcskei, R.U. Nabar, O. Oyman, and A.J. Paulraj, "Capacity scaling laws in mimo relay networks," *IEEE Trans. Wireless Commun.*, vol. 5, no. 6, pp. 1433–1444, June 2006.

[4] N. Ida, *Engineering Electromagnetics, 2nd Edition*, Springer, May 2004.

[5] Theodore S.Rappaport, *Wireless Communications Principles and Practice, 2nd Edition*, Communications Engineering and Emerging Technologies. Prentice Hall, 2002.

[6] T. M. Cover and J. A. Thomas, *Elements of Information Theory, 2nd Edition*, Wiley-Interscience, July 2006.

[7] R.M. Gray, "Toeplitz and circulant matrices: A review," in *Foundations and Trends in Communications and Information Theory*, vol. 2, pp. 155–239. NOW, the essence of knowledge, Stanford University, 2006.